Heat Flow through Winter Ice*

E. L. LEWIS

Bedford Institute of Oceanography, Department of Energy, Mines and Resources, Dartmouth N. S., Canada

Abstract

Temperature measurements have been made at vertical intervals of 15 cm in a growing sea ice sheet to an accuracy of ±0.01°C at hourly intervals for over 800 hours. Five such profiles were recorded simultaneously together with ice thickness and temperature structure of the underlying water. Assuming a value for the latent heat of formation of sea ice, the total heat flow into the ice at its lower surface is determined and is related to the heat flow from the upper surface of the ice at an earlier time. Values for the thermal conductivity of sea ice as a function of temperature are given and compared to those predicted by model studies.

I. Introduction

Heat flow through sea ice has received considerable previous attention in connection with studies of energy exchange between the upper surface of the ice or snow cover and the atmosphere. Schwerdtfeger and Pounder (1963) discuss the energy flow away from the surface during the winter and spring. Untersteiner (1961, 1964 a) and Vowinckel (1964) have been concerned with the overall energy balance throughout the year. The present study is directed towards the lower surface of the ice to obtain an understanding of the energy exchange between the ocean and the ice sheet and the manner of transmission of the energy through the ice to its upper surface.

During ice growth the heat flow through the ice sheet in response to the temperature difference between upper and lower surfaces may be conveniently divided into four components due, respectively, to changes in the internal energy of the sheet, to the latent heat liberated at the growing interface by ice accretion, to the sensible heat exchange with the underlying ocean, and to net radiative heat exchange within the ice sheet. The work of Kelley, Bailey and Lieske (1962) shows that the radiation term is nearly zero during the months of January and February at a latitude of 71°N even in the absence of a snow cover, and using the extinction coefficient of about 1.4 given by Mellor (1965) for fine grain snow, the presence of a centimeter of snow at that time will certainly give it a value far below the level of observations. As the experiment to be described was conducted at Cambridge Bay, N.W.T. (69°04'N 105°00'W) during the early part of the year under an irregular snow cover of up to 40 cm, radiation may be neglected. Thus in the present case the heat flow may be considered to be the sum of three components, two

* Contribution No. 62, Bedford Institute of Oceanography.

of which, latent and sensible heat, are physically identifiable and measurable at the ice-water interface and a third, internal energy change, which is usually of concern at the upper surface of the ice where it represents the net internal energy change within the whole ice sheet. All these components, however, may be defined to have values at any point within the ice and it is convenient to write at depth z from the upper surface at any time t,

$$Q(z,t)=Q_{\mathrm{L}}(z,t)+Q_{\mathrm{o}}(z,t)+Q_{\mathrm{u}}(z,t)\,, \tag{1}$$

where $Q(z,t)$ is the total heat flow per unit area and time, $Q_{\mathrm{L}}(z,t)$ the component associated with the liberation of latent heat at the growing interface $z=S$, $Q_{\mathrm{o}}(z,t)$ the component associated with flow of sensible heat from the ocean to the ice, and $Q_{\mathrm{u}}(z,t)$ the heat flow associated with changes of stored energy in the ice sheet. A special case of eq. (1) is

$$Q(S,t)=Q_{\mathrm{L}}(S,t)+Q_{\mathrm{o}}(S,t)\,, \tag{2}$$

for if the ice is growing $Q_{\mathrm{u}}(S,t)$ is identically zero by definition.

The study of heat flow through the ice now falls into two parts: determination of the factors on the right hand side of eq. (2) from experimental observations, and determination of the proper relationship between $Q(S,t)$ and $Q(z,t)$ allowing the latter to be seen as the cause of the former. These two points will be dealt with in turn.

$Q_{\mathrm{L}}(S,t)$ may be evaluated from knowledge of the latent heat of formation of sea ice and the accretion rate of the ice sheet. To determine $Q_{\mathrm{o}}(S,t)$ it is necessary that the water under the ice sheet should respond to ice growth alone without the introduction of extraneous and unknown sources or sinks of heat. Cambridge Bay was chosen as a site for the experiment because of extremely stable water conditions and an almost complete absence of advection currents. The Bay, of area 8 km^2 approximately and maximum depth 75 m, is connected to the open sea by a passage of length 14 km and minimum width 1.2 km containing 3 sills of depths 15 m or less. The sills are in turn separated by shallow basins which serve to make tidal water enter and leave the Bay more or less uniformly across the passage. The water is essentially homogeneous, at least to the depth of the sills, when it would appear that tidal waters would flow in and out almost down to the depth of the sill. Using this assumption, the movement of a given water particle 300 m to and fro in the narrowest part of the passage would constitute the average diurnal tide, which has a height difference of 40 cm. The above discussion applies to Cambridge Bay during the nine months or more of the year when it is ice covered and has been substantiated by detailed oceanographic surveys not reported herein. Thus the structure of the water column underlying the growing ice sheet on the Bay is that due to convective processes acting on the structure existing at the time of freeze-up.

A physically instructive method of connecting the heat flow at the upper surface to the heat flow into the growing interface is to consider the propagation of heat through the ice sheet. A flux $Q(0,t_1)$ at the surface at time t_1 progresses downwards and is attenuated until at the interface a heat flow of $Q(S,t_2)$ remains where $t_2>t_1$. $Q(S,t_2)$ then produces the observed ice growth and sensible heat exchange at $z=S$; the attenuation with increasing z is due to the production of changes in the internal energy of the ice sheet. To make the connection between the Q's it is necessary to determine the curve in the (z, t) plane along which heat may be thought to flow. For the case of arbiterary surface temperature fluctuations as met in nature this is a point of some complexity, and must be discussed in detail.

A relationship between heat fluxes at different depths and times may be derived from solution of the appropriate thermal diffusion equation for given boundary conditions. A solution of this type using the simple diffusion equation (*i.e.* thermal "constants" constant) is shown in Fig. 9. Little physical insight is obtained from this calculation. Another approach is to replace the growing ice sheet by a finite slab of sea ice whose upper and lower surfaces coincide with those of the growing ice at the time of interest. Analysis of the slab gives a good approximation to actuality for ice of thickness greater than 50 cm for then the increase in ice thickness during the time required for transmission of thermal energy through the ice may be thought negligible. With a constant surface temperature the predicted temperature profile for the growing sheet is linear well within the limits experimentally observable in the present case and so corresponds to the slab. The approximation may be used for periods of time short compared to those required for a significant change in the "linear" temperature profile due to accretion. Reference for the above statements and for the following discussion is made to the standard text of Carslaw and Jaeger (1959). A solution of the simple thermal diffusion equation in closed form is available for the finite slab with a sinusoidal temperature variation at the upper surface and the lower surface kept at constant temperature. Computations based on this solution using constants suitable for sea ice indicate that for a slab thickness of greater than 50 cm the slab may be replaced by a semi-infinite body whose boundary coincides with the upper boundary of the slab with negligible change in the predicted temperature profile. Thus for an approximate study of the propagation of temperature fluctuations thick sea ice may be replaced by a semi-infinite body, which is equivalent to saying that the reflection of temperature waves from the lower surface of the ice is negligible.

For the homogeneous semi-infinite body subject to the surface temperature $T(0, t) = A \cos \omega t$ the steady state solution for the temperature at any depth and time is

$$T(z, t) = A \exp(-\gamma z) \cos(\omega t - \gamma z),$$

where $\gamma = (\omega/2K)^{\frac{1}{2}}$, K being the thermal diffusivity. It is noted that the amplitude of temperature fluctuations suffers an exponential attenuation with depth and that points of constant phase are on a straight line of slope $\omega/\gamma = (2\omega K)^{\frac{1}{2}}$ in the (z, t) plane. It is possible to conduct a spectral analysis of the naturally occurring surface temperature fluctuations and find a solution for $T(z, t)$ as a summation of terms of the type shown above. Component frequencies of the spectrum may be classified in terms of a characteristic frequency ω_c, defined as the frequency at which the ice sheet is one wavelength thick. From the above $\omega_c = 8\pi^2 K/S^2$; a component at this frequency is attenuated to $\exp(-2\pi) = 1.9 \times 10^{-3}$ of its surface value by passage through the ice. Components at frequencies significantly greater than ω_c have very little effect on ice growth as they are attenuated to a negligible level before reaching the interface. Components at frequencies significantly below ω_c cause comparatively slow variations in growth conditions and provide a nearly constant component of heat flow during short term fluctuations. The phase of these very low frequency components may be considered constant during the transit of components of frequencies near ω_c. Components at frequencies near ω_c cause noticeable short term variations in ice growth. A practical instance for the application of this division of frequency components is shown in Fig. 2 (curve labelled (30.0)) which represents the ice surface temperature variations with time. It is noted that small high frequency peaks are superimposed on larger variations extending over 50 to 100 hours which are in turn superimposed on a very low frequency variation extending across the graph. Thus for an approximate study of the relation between surface heat flow fluctuations and growth rate variations over periods of the order of ω_c attention may be confined to a band of frequency components around ω_c. The final approximation is to allow a single propagation velocity to characterize all frequencies within this band. It is noted from the above that a variation of velocity with $\omega^{\frac{1}{2}}$ is predicted.

It is now possible to define a curve $z=f(t)$ in the (z, t) plane corresponding to the constant phase curve for the monochromatic idealization. This curve represents the locus of all significant temperature fluctuations progressing from the surface to the growing interface. For example, attention may be directed to a maximum of surface temperature and this maximum traced through the ice sheet from temperature profile data to give $z=f(t)$. At the maximum $\partial T/\partial t=0$ and at that point, from the thermal diffusion equation, $\partial T/\partial z$ has an extremum value. Hence $z=f(t)$ is also the locus of heat flow variations down through the ice sheet and so enables the Q's of eqs. (1) and (2) to be connected.

It is to be emphasised that $z=f(t)$, when derived from given experimental data is good only for that data unless an extension to other data can be justified by comparison of natural conditions prevailing in each case. Support to the use of the technique in the present instance is lent by consideration of Fig. 3 which compares surface temperature fluctuations and values of temperature gradient at the growing interface. It is seen that the time interval between the existence of temperature maxima at the upper surface and the arrival of the corresponding gradients at the interface is constant within a few per cent at 87 hours. The period of the characteristic frequency for this case, found by using an average value for $K(8.5\times10^{-3}\,\mathrm{cm^2/sec})$ is 71 hours.

On the curve $z=f(t)$, $Q_L(z, t)$ and $Q_0(z, t)$ are invariant so that eqs. (1) and (2) may be combined and written

$$Q(z_1, t_1)=Q(S, t_2)+Q_u(z_1, t_1), \tag{3}$$

where (z_1, t_1), (S, t_2) are points on $z=f(t)$. Also

$$\delta Q_u=\delta Q=\frac{\partial Q}{\partial z}\,\delta z+\frac{\partial Q}{\partial t}\,\delta t \;\; (z=f(t)).$$

Thus

$$Q(z_1, t_1)=Q(S, t_2)+\int_C\left[\frac{\partial Q}{\partial z}\,\delta z+\frac{\partial Q}{\partial t}\,\delta t\right], \tag{4}$$

is being understood that the line integral is taken along $z=f(t)$ from (S, t_2) to (z_1, t_1). The integral may be evaluated numerically as is shown in section III-4 from knowledge of temperature distributions within the ice sheet. Equation (4) connects the heat flow into the growing interface with that existing at a higher level (in particular at the surface) at an earlier time in a "cause and effect" relationship and so allows prediction of heat loss to the atmosphere in terms of ice growth. Equation (4) is an approximation, the validity of which depends on the accuracy in any given case of the assumptions made in order to define $z=f(t)$. It will be least accurate near the ice surface where high frequency temperature components have not been attenunated to a negligible level. However, as will be seen, it provides a quick and easy method of prediction of heat flow from the mean data usually availabe from weather stations with, it is believed, a considerably higher order of accuracy than has heretofore been available.

II. The Experiment

Five thermistor chains, each consisting of thirteen thermistors 15 cm apart, were put into the ice along a straight line at intervals of 10 m. Ten days were allowed after insertion before any measurements were made which, from results reported later, appears adequate for temporary temperature perturbations caused by insertion to decay to negligible proportions. Disturbances in snow cover above the chains were also removed by winds during this period. The chains were connected to an automatic data logging system in a heated hut by cables lying on the surface of the snow. Values for the voltage drop across the thermistors when switched sequentially into this circuit by a scanning unit were measured by a digital voltmeter and recorded on both punched and printed paper tape. A complete scan of all inputs was made every hour and took approximately three minutes. From the freezing point down to $-10°C$ it is considered that the measurement of temperatures was accurate to at least $\pm 0.01°C$ and at lower temperatures differences between true values and those recorded were constant within $\pm 0.01°C$. Temperature measurements of this accuracy if applied to the calculation of temperature gradients require precise positioning of the thermistor. A typical vertical temperature gradient in the ice sheet was $0.15°C/cm$ or $\pm 0.01°C$ in ± 0.66 mm. It is considered that the thermistors were positioned within ± 0.5 mm though inevitably the chains were subject to some mechanical strain during insertion.

Ice thickness measurements were made partly by conventional drilling techniques and partly by use of a technique suggested by Untersteiner (1964 b). Rods, 2 m long 5 mm in diameter consisting of closed stainless steel tubes surrounding nichrome heaters embedded in an insulating refractory oxide were placed vertically through the ice sheet. These rods or "wands" had crossbars attached to their lower ends and, upon release from the ice by application of power to the heater, could be lifted until the crossbar touched the ice. This gave the ice thickness. Ice thickness measurements as shown on Fig. 1 are considered accurate to ± 0.5 cm.

Temperature profiles of the waters underlying the ice sheet were made by measurement of the resistance of a thermistor lowered into the water by means of a special winch, and are accurate within $\pm 0.01°C$. The salinity profile of the ice sheet was determined by use of a hydrometer to measure the salinity of solutions resulting from the melting of specimens of ice taken from given depths in the sheet. Values are shown on Fig. 8.

A full description of the techniques used in the experiment will be published elsewhere.

III. Results and Discussion

1. *General Description.* Figure 1 shows the location of the five thermistor chains along the base line in relation to ice-water profiles. Chains are subsequently referred to by their position on this figure so that "chain 20" occupies the 20 m position. It is apparent that variations in thickness of up to 15% are a permanent feature of the ice cover in Cambridge Bay. These variations are tentatively ascribed to corresponding variations in snow cover but this could not be substantiated experimentally due to the frequent movement of drifts in high winds. The smoothed ice-water interface profiles have a maximum inclination to the horizontal of 1°37′, but surface irregularities could cause much greater inclinations to exist over short distances, a variation in thickness equivalent to 1 cm in 8 cm horizontal separation being common. These results indicate the difficulties involved in attempting accurate incremental ice thickness measurements by means of conventional ice drilling techniques. If sequential measurements are made at the same location, all results other than the first are liable to error due to perturbations in heat flow resulting from the initial drilling, unless the time intervals between readings is great. If different locations are used any rate of growth up to a given maximum may be found. In the present instance zero growth over a month could be recorded. Slender electrically heated rods as described in section II give good values for values for incremental thicknesses provided that a sufficient time interval is taken to make the limits of accuracy as applied to the two readings unimportant as a percentage of the difference recorded. However, such rods cannot, for obvious reasons, be placed immediately adjacent to sensitive thermistor chains so that values for temperature cannot be properly connected to thickness data.

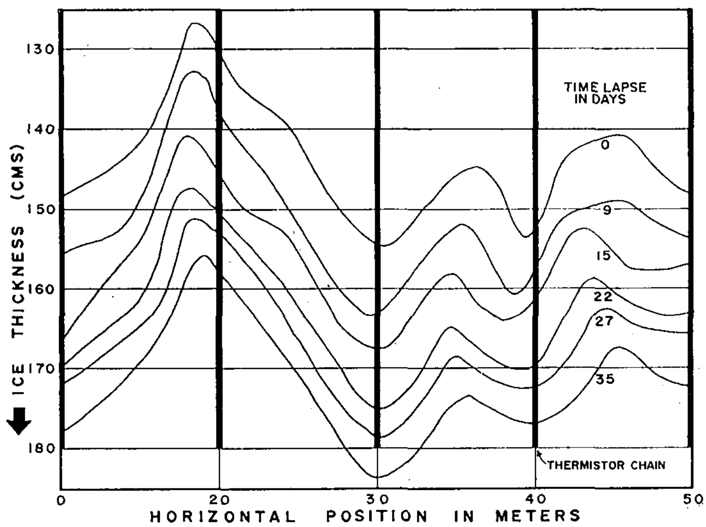

Fig. 1. Profiles of ice-water interface showing variation with time, and position of thermistor chains

Figure 1 shows that over the entire 35 days the ice grew about 29 cm in the vicinity of chan 30 and about 28 cm in the vicinity of chain 20. Temperature readings from these two chains, which are respectively near the thickest and thinnest portions of the ice sheet, indicate that the vertical temperature gradient measured in the ice at its surface is at least twenty five times as great as the maximum horizontal temperature gradient. As a consequence of the essentially uniform growth and the absence of large horizontal gradients it is considered that a one dimensional analysis of heat flow may be applied to the data without causing significant errors in relation to the stated ±0.01°C accuracy of temperature measurement.

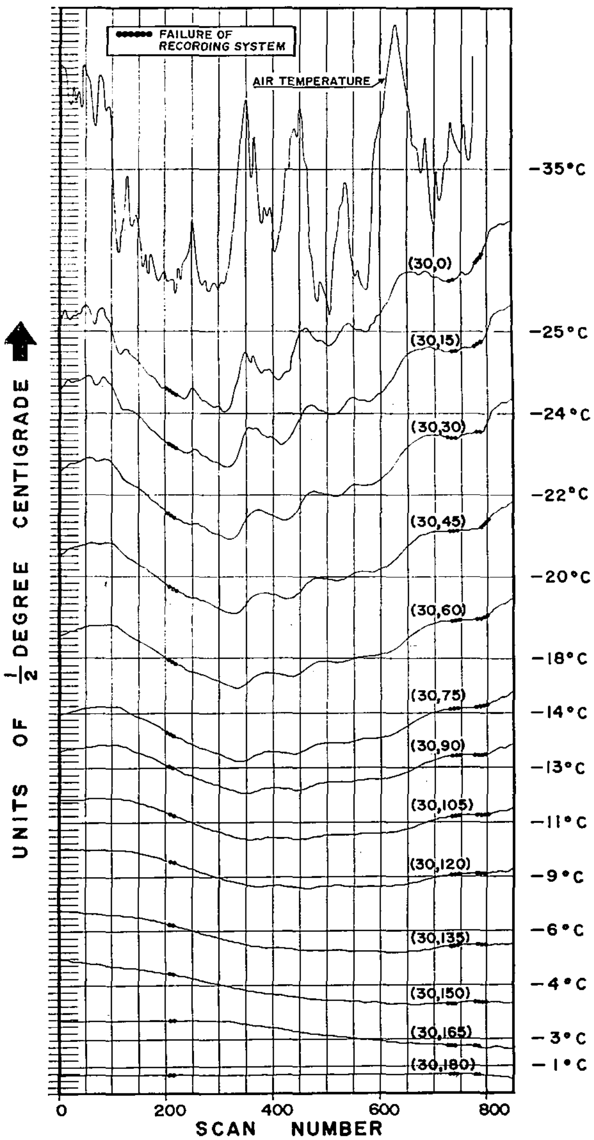

Fig. 2. Temperature variation with scan number (*i.e.* time in hours) at 15 cm intervals in sea ice sheet. Air temperature is also shown

Figure 2 shows a complete set of temperature records from chain 30 over the entire period of over 800 scans. Similar records are available for all the other chains. The scan number is equivalent to elapsed time in hours and the graph covers the entire growth period shown in Fig. 1. The curves are labelled to show the co-ordinate position of the thermistor indicating that temperature. Thus (30, 105) indicates in meters and centimeters respectively the position of the chain referred to and the depth of the thermistor below the surface of the ice. The top curve on Fig. 2 labelled "air temperature" is from the records of the Department of Transport Meteorological Station at Cambridge Bay and this allows comparison of temperature-time profiles from two independent measurement systems. It is noted that the degree of detail reflected in (30, 0) as a result of the changing air temperature varies. This is the result of alterations in snow cover and on large scale plots it is possible to see that the time lag between corresponding features on the two curves has increased from 1 hour around scan 65 to 3 hours around scan 400 to 7 hours around scan 530.

2. *Heat flow at the growing interface.* As described in section I the heat flow into the ice at the ice-water interface consists of two components, $Q_L(S, t)$ due to the liberation of latent heat and $Q_0(S, t)$ due to transfer of sensible heat from the ocean to the ice.

In order to obtain values for $Q_L(S, t)$ it is necessary to know the latent heat of formation of sea ice L, its density, ρ, and the rate of accretion dS/dt. No experimental measurements determining L at the interface are known and the best available value is due to Schwerdtfeger (1963) who calculates that $L = 67.5$ cal/g for sea ice of 5‰ salinity. This value is based on the assumption that the pockets of brine entrapped in the ice during growth, which give rise to the overall salinity of the sea ice, have an individual salinity equal to that of the sea. The assumption is incorrect as has been pointed out by Pounder (1965) but it is thought that the error thereby introduced is probably small. Experimental values for density are available from a number of authors and appear quite consistent. Schwerdtfeger's value of 0.915 g/cc will be used herein.

The inadequacy of conventional ice thickness measurements for accurate determination of dS/dt has already been discussed. A least squares quadratic approximation of the temperature profile near the interface was constructed using values of temperature at the four levels nearest the interface. The z co-ordinate of the intersection of this approximate profile with the line $T = -1.56°C$ was taken as the interface position. It is probable that the line $T = -1.57°C$ would have been a better choice but the error, if any, is consistent and merely shifts values for S by about 0.06 cm. The standard deviation of the approximation was in nearly all cases less than 0.01°C, the calculation being carried out at intervals of 5 hours for all the data from the lower levels of chain 30 shown on Fig. 2. This figure also shows that (30, 165) was enveloped by the ice at scan 312 so that the four points used to produce the approximation were changed at that time. Immediately following scan 312 the result for the interface position will be accurate to at least ± 0.1 cm so that at an approximate growth rates of 0.035 cm/hour, as given by Fig. 1, averaging over 50 hours would allow an average value of dS/dt to be calculated to an accuracy of $\pm 5\%$. A still better method, which gives time dependent values of dS/dt, is to use the relation, true on any isothermal and so at the interface, that

$$\frac{\mathrm{d}S}{\mathrm{d}t} = -\left[\frac{\partial T/\partial t}{\partial T/\partial z}\right]_{z=S},$$

$(\partial T/\partial z)_{z=S}$ is found from the least square quadratic approximation to a high degree of accuracy as the profile near the interface departs from linear by a small amount only. $(\partial T/\partial t)_{z=S}$ may be found from plots of temperature versus time as a thermistor goes into the ice, (30, 165) at scan 312 being an example.

Figure 3 shows (30, 0), $(\partial T/\partial z)_{z=S}$ and S against scan number, the last two functions being calculated as described above and the first being transferred directly from Fig. 2. It will be noted that there is a break in the two lower curves at scan 312 where the changeover of levels used to obtain the tleas squares approximation is made. The gradient suffers a change of 0.006°C/cm or 3.6% and the thickness a change of 0.5 cm or 3.3% of the 15 cm distance the temperature profile had been projected from the (30, 150) reading which was that nearest the interface for the left hand curve. Regarding the curve for (30, 0) and $(\partial T/\partial z)_{z=S}$ on Fig. 3 it is apparent that the general features of the surface temperature may be seen, displaced in time, on the gradient curve. Most prominant is the isolated temperature maximum at scan 248 reflected as a minimum gradient

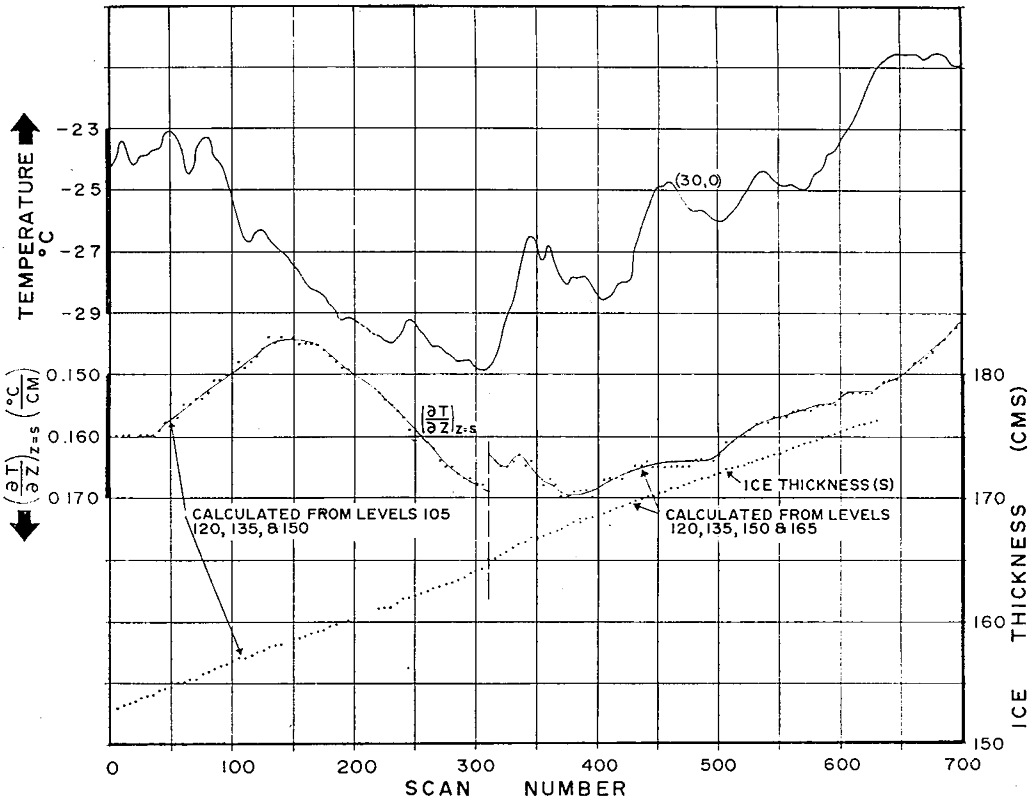

Fig. 3. Relation between (30, 0) temperature record, temperature gradient at growing interface, and ice thickness S. Calculated values are derived from least squares approximation of temperatures at levels shown

at scan 335. Other recognisable features hold to this time lag approximately. Comparison of curves of this type provided the basis for Fig. 7.

Figure 4 shows plots of temperature at thermistors (30, 165), (40, 165) and (50, 165) as these thermistors moved from the sea into the ice sheet. Values for $(\partial T/\partial t)_{z=S}$ are given on the figure. Values of $(\partial T/\partial z)_{z=S}$, $(\partial T/\partial t)_{z=S}$ and $\mathrm{d}S/\mathrm{d}t$ are tabulated in Table 1 for chains 10, 30, 40 and 50. Values for $Q_L(S, t)$ calculated from these results are also given. The data for chain 10 must be considered less reliable than that for the other chains because of some instability noticeable in the time-temperature curve of (10, 165) as the ice grew around it. An average value of $(\partial T/\partial t)_{z=S}$ has been taken.

Sensible heat flow from the sea to the ice appears to have been neglected or considered negligible in comparison to the latent heat term by previous authors. The present

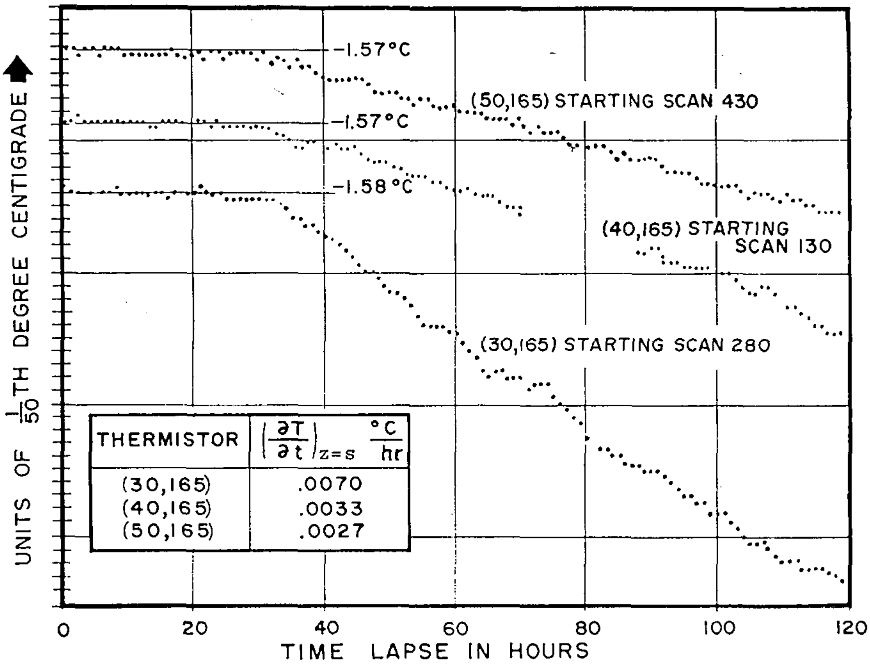

Fig. 4. Curves showing rate of change of temperature with time as thermistor is enveloped by the growing ice sheet

Table 1.

$S = 165$ cm $L = 67.5$ cal/g $\rho = 0.915$ g/cc

Chain No.	hour	$\frac{°C}{cm}$	$\frac{°C}{hr}$	$\frac{cm}{hr}$	$\frac{cal}{cm^2 \cdot hr}$	$\frac{cal}{cm^2 \cdot hr}$	$\frac{cal}{cm^2 \cdot hr}$	c.g.s. units $\times 10^3$
	t	$\left[\frac{\partial T}{\partial z}\right]_{z=S}$	$\left[\frac{\partial T}{\partial t}\right]_{z=S}$	$\left[\frac{dS}{dt}\right]$	$Q_L(S, t)$	Q_0	$Q(S, t)$	k
10	185	0.142	−0.0052	0.036	2.22	0.2	2.42	4.7
30	312	0.163	−0.0070	0.043	2.65	0.2	2.85	4.8
40	164	0.121	−0.0033	0.027	1.67	0.2	1.87	4.3
50	440	0.114	−0.0027	0.024	1.48	0.2	1.68	4.0

study indicates that about 10% of the total heat flow has its source in the ocean. The exact mechanism of this convective process is not known but its gross effects may be observed in the structure of the sea water column underlying the ice sheet. Figure 5 shows temperature profiles in the waters of Cambridge Bay which have as their most significant feature an abrupt temperature change at a depth of 20~30 m. It is to be noted from the figure that the position of this change has fallen about 3 m in 23 days. Curves of identical shape to either of those shown in Fig. 5 could be found at any position in Cambridge Bay on the given date, cut off at the depth of the Bay at the place of measurement. Internal waves exist in the system and the measuring thermistor, when placed at the level of the temperature jump, showed fluctuations in readings corresponding to a wave amplitude (peak to peak) of about 1 m. The curves of Fig. 5 are average curves based on a series of readings in an attempt to obtain a mean position in the presence of the internal waves.

The absence of advection currents in Cambridge Bay has already been discussed and it is this fact that enables the profiles of Fig. 5 to be related to the convective processes occurring under the ice sheet. Surveys not reported herein but conducted throughout a season of ice growth show a gradual but steady fall in the position of the temperature jump which is the limit of convective penetration into the water structure left from the preceding summer. In the author's opinion temperature profiles similar to those of Fig. 5 exist under all growing sea ice except where perturbed by currents.

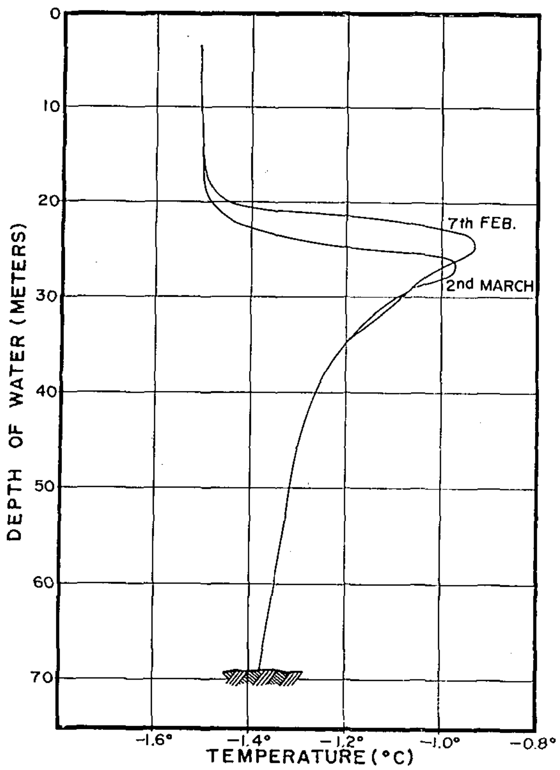

Fig. 5. Temperature profiles of water underlying ice sheet

The oceanographic data given by Brayton (1962) taken from the Arlis I ice island in 1960 and 1961 shows many bathytherymograph records similar to Fig. 5. It may be considered that other records not following Fig. 5 could be the result of currents at that station.

Taking the specific heat of sea water as 0.946 cal/g·°C which is appropriate for water of salinity 28‰ near its freezing point, the data of Fig. 5 shows that about 120 cal were removed from the sea per square centimeter of cross sectional area over 23 days. This corresponds to an average heat flow from the ocean of about 0.2 cal/cm^2/hour. As the sea water temperature profiles of necessity average out any variations in convective processes with ice thickness the taking of this value of heat flow as equal to $Q_0(S, t)$ means that the function could be properly written as Q_0, a constant for the period of the experiment. As no better alternative exists the values of 0.2 cal/cm^2/hour is entered in Table 1 and allows calculation of $Q(S, t)$ from which in turn values for the thermal conductivity of ice, k, at the growing interface may be calculated. It is considered that the main source of error in the calculations is the degree of uncertainty in the value for $(\partial T/\partial t)$. This quantity was determined many times from the data of Fig. 4 by various methods and is considered to be accurate within $\pm 3\%$. Values for thermal conductivity are then to an accuracy of $\pm 0.1\times 10^{-3}$ c.g.s. units. The data for chain 10 is less reliable.

3. *Propagation of temperature changes through the ice sheet.* Figure 6 is a large scale plot of a small section of Fig. 2 and shows the propagation of a rapid variation

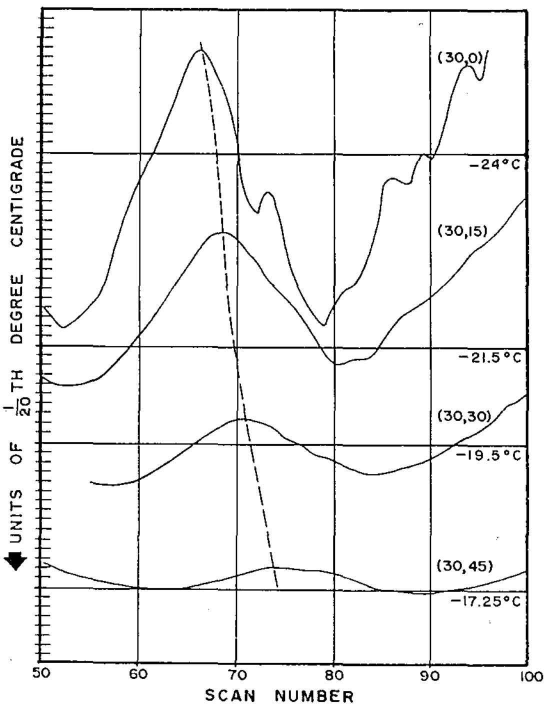

Fig. 6. Detail of a section of Fig. 2 showing propagation of temperature variations from the surface down to the 45 cm level

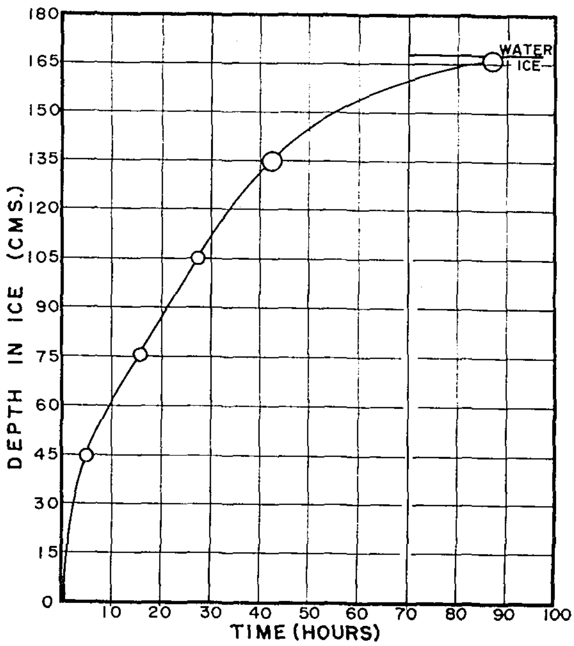

Fig. 7. *Propagation of temperature gradient minimum through the ice sheet.* Size of circles represents degree of uncertainty of position of point

in surface temperature down to the 45 cm level. It is seen that the amplitude of the temperature variation decreases with depth until, at the 45 cm level, it is difficult to locate precisely the position of the temperature minimum indicated on the figure by the intersection of a dotted line and the temperature-time wave. In addition to this amplitude reduction precise location of temperature minima (or maxima) deep in the ice is dependent on the absence of secondary variations in the vicinity of the minimum chosen. This effect is illustrated by the rapid degeneration of the maximum at scan 79 level 0 cm (Fig. 6) as a result of the point of inflexion existing at scan 81–82 on the same curve. The ideal situation in which to identify propagation of temperature variations into the ice sheet is where a smooth fluctuation exists.

This ideal is most nearly realized in the present instance by the maximum to be seen at scan 248, level 0 on Fig. 2 which, though less sharp than that used in Fig. 6, is quite "clean". It is possible to trace this temperature maximum through the ice sheet to the growing interface. It has been shown in section I that the temperature maximum is an extremum of $\partial T/\partial z$. This extremum is a minimum and Fig. 7 is a plot of the time at which it reaches given depths in the ice sheet taking time as zero at the upper surface. Figure 7 has been derived from plots similar to Fig. 3; the curve has the equation $z=f(t)$ referred to in section I.

4. *Heat flow through the ice sheet.* The process of transmission of heat through the ice sheet may now be described in terms of the interface heat flow, $Q(S, t)$ and $z=f(t)$. The result for chain 30 as given in Table 1 will be used as an example.

From Fig. 7 it is seen that 87 hours are required for the penetration of a given temperature gradient variation through an ice sheet 165 cm thick. Thermistor (30, 165) entered the ice at 312 hours so that the heat flow, $Q(165, 312)$ at the interface corresponds to $Q(0, 225)$ at the upper surface of the ice. At that time a gradient of 0.202°C/cm existed at the surface (determined from the data plotted in Fig. 2). Following back down $z=f(t)$ it is seen that $Q(0, 225)$ corresponds to $Q(45, 232)$ at 0.179°C/cm, to $Q(90, 247)$ at 0.177°C/cm, and so on back down to $Q(165, 312)=2.85$ cal/cm²/hr at 0.163 °C/cm, these last two numerical values being taken from Table 1. To determine the value of $Q(S, t)$ at any point on $z=f(t)$ eqs. (3) and (4) are used which, for this particular case, read

$$Q(z, t)=2.85+Q_{\mathrm{u}}(z, t),$$

$$Q_{\mathrm{u}}(z, t)=\int_C\left[\frac{\partial Q}{\partial z}\,\delta z+\frac{\partial Q}{\partial t}\,\delta t\right],$$

the line integral being taken from the growing interface up to (z, t) along the curve.

The thermal diffusion equation may be written

$$\frac{\partial Q}{\partial z}=\rho C\frac{\partial T}{\partial t},$$

where C is specific heat, and

$$\frac{\partial Q}{\partial t}=k\frac{\partial}{\partial t}\left[\frac{\partial T}{\partial z}\right],$$

where k is thermaln coudctivity. Thus

$$Q_{\mathrm{u}}(z, t)=\int_C\left[\rho C\frac{\partial T}{\partial t}\,\delta z+k\frac{\partial}{\partial t}\left[\frac{\partial T}{\partial z}\right]\delta t\right].$$

In the present case where temperatures are available at 15 cm intervals, the line integral is replaced by a summation in steps using average values for the variables. Carrying out this procedure for each term to be integrated gives, for the first 15 cm step up from the interface

$$\int_C\rho C\frac{\partial T}{\partial t}\,\delta z=\delta z\,\bar{C}\rho\left[\frac{\partial T}{\partial t}\right]_{\mathrm{Av}}=15\,\frac{\bar{C}\rho}{2}\left[\left[\frac{\partial T}{\partial t}\right]_{165,312}+\left[\frac{\partial T}{\partial t}\right]_{150,280}\right],$$

and

$$\int_C k\frac{\partial}{\partial t}\left[\frac{\partial T}{\partial z}\right]\delta t=\delta t\,\bar{k}\,\frac{\partial}{\partial t}\left[\frac{\partial T}{\partial z}\right]_{\mathrm{Av}}=\frac{32\bar{k}}{2}\left[\frac{\partial}{\partial t}\left[\frac{\partial T}{\partial z}\right]_{165,312}+\frac{\partial}{\partial t}\left[\frac{\partial T}{\partial z}\right]_{150,280}\right],$$

as (165, 312), (150, 280) are, respectively the coordinates on $z=f(t)$ of the interface and the point 15 cm above the interface. $\bar{C}$ and $\bar{k}$ are the average specific heat and thermal conductivity. Addition of the above two factors gives $Q_{\mathrm{u}}(150, 280)$. The summation may now be taken over the next step to give $Q_{\mathrm{u}}(135, 267)$ and so on up to $Q_{\mathrm{u}}(0, 225)$.

The calculation for the given case of chain 30 is tabulated in Table 2 to which reference is made. Values for z and t give coordinates of points on the curve of Fig. 7, referred to a time origin of 225 hours. Values for $(\partial T/\partial t)$ have been obtained by averaging over a period of 4 hours or more centred on the appropriate value of t. They are thought to be accurate within ±0.001°C/hour, this estimate being based on the typical departure from a smooth curve when $(\partial T/\partial t)$ is plotted over a period of time. It should be noted that acceptance of values for $(\partial T/\partial t)$ at the accuracy quoted demands a stability of temperature measurement rather than accuracy of temperature

Table 2.

cm	hour	°C	$\frac{°C}{cm}$	$\frac{°C}{hr}$	$\frac{°C}{cm \cdot hr} \times 10^5$	$\frac{cal}{g \cdot °C}$	$\frac{cal}{cm^2 \cdot hr}$	$\frac{cal}{cm^2 \cdot hr}$	c.g.s. $\times 10^3$
z	t	$T(z, t)$	$\left[\frac{\partial T}{\partial z}\right]_{z,t}$	$\left[\frac{\partial T}{\partial t}\right]_{z,t}$	$\frac{\partial}{\partial t}\left[\frac{\partial T}{\partial z}\right]_{z,t}$	$\bar{C}$	$Q_u(z, t)$	$Q(z, t)$	k
0	225	−30.85	0.202	−0.040	36	0.45	1.7	4.55	6.2
15	227	−26.87	0.197	−0.030	105	0.45	1.5	4.35	6.1
30	229	−24.00	0.187	−0.020	30	0.46	1.3	4.15	6.1
45	232	−21.37	0.179	−0.022	5	0.46	1.2	4.05	6.2
60	235	−18.84	0.176	−0.019	3.5	0.48	1.1	3.95	6.2
75	241	−16.25	0.180	−0.019	3	0.49	0.97	3.80	5.9
90	247	−13.64	0.177	−0.016	1.5	0.53	0.86	3.70	5.8
105	252	−11.12	0.173	−0.015	3	0.57	0.74	3.60	5.8
120	259	− 8.60	0.170	−0.011	7	0.75	0.64	3.50	5.7
135	267	− 6.18	0.168	−0.010	11	1.40	0.52	3.35	5.5
150	280	− 3.75	0.167	−0.008	10	2.50	0.33	3.15	5.2
165	312	− 1.58	0.163	−0.007	20		0.00	2.85	4.8

measurement. It is quite possible that the value for $T(0, t)$ has a consistent error of 0.02°C which will not affect values for $(\partial T/\partial t)$. However due to the uncertainty within a few hours of which scan to take in order to compute $(\partial T/\partial t)$, values for the upper levels in the ice, where $(\partial^2 T/\partial t^2)$ has a significant value, may be in error. The main reason for using the chain 30 data for the specimen calculation was that the surface

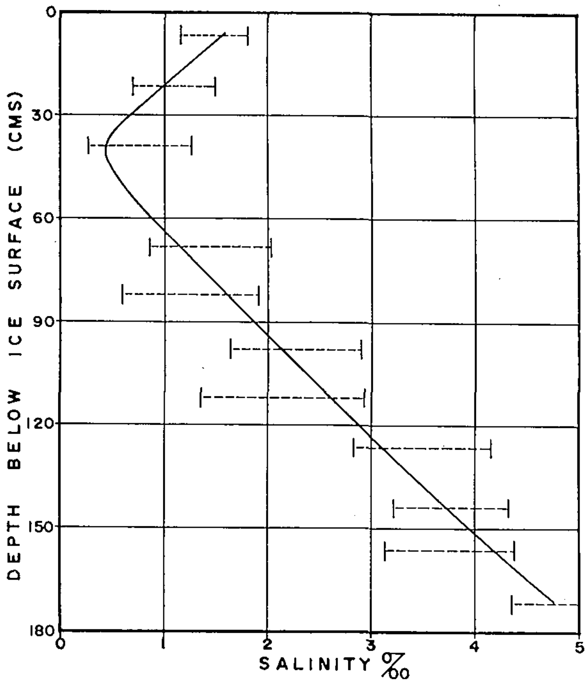

Fig. 8. Salinity profile of ice sheet. Curve is smoothed out plot of average of four determinations at each depth. Range of values is shown by limit marks

temperature showed a steady change with time at the appropriate scan number. C has been measured and tabulated as a function of temperature and salinity by Schwerdtfeger (1963) and is taken from his table using $T(z, t)$ and salinity (Fig. 8) to determine the value. Values for C down to $-23°C$ are given: below that temperature an extrapolation has been made which is of very doubtful validity due to the precipitation of the salt $NaCl \cdot 2H_2O$ in the brine pockets of the ice at $-22.9°C$. Values for $\partial T/\partial z$ and $\partial/\partial t$ $(\partial T/\partial z)$ are taken from the raw data as shown in Fig. 2. The former are probably accurate within $\pm 0.001°C/cm$ and the latter within $\pm 10\%$. $\bar{k}$ is taken as 4.8×10^{-3} c.g.s. units near the growing interface and 6.0×10^{-3} c.g.s. units near the upper surface. It is most fortunate that neither $\partial/\partial t(\partial T/\partial z)$ nor $\bar{k}$ need to be known accurately as the component of the summation involving these quantities is very small compared to the specific heat term. The contribution from the $\bar{k}$ term is insignificant except near the upper surface where it equals one eighth of the total value of the summation step and near the growing interface where, due to the length of the interval t, (32 hours) it is about one quarter of the total. Values for $Q_u(z, t)$, $Q(z, t)$ and k follow as the previously assumed value for $\bar{k}$ has negligible effect on k if it is varied by $\pm 25\%$.

It is seen that a heat flow of 4.55 cal/cm²/hour emerging from the ice surface gives rise to a cooling of the ice sheet requiring 1.7 cal/cm²/hr, an ice growth of 0.043 cm/hr requiring 2.65 cal/cm²/hr, and a heat exchange with the ocean of 0.2 cal/cm²/hr.

5. *Approximate values for heat flow.* The above evaluation of heat flow is not of general practical application owing to the extent of data necessary for the calculation. A frequent requirement is to be able to evaluate heat flow from knowledge of surface temperature mean values and ice thickness which are usually available from Meteorological Station Observations. Consider then an ice sheet of thickness S having a constant differential temperature T_0 between its upper and lower surfaces. For ice of thickness greater than 50 cm there is little error in assuming the temperature gradient to be constant as has been discussed in section I. The heat flow from the ice surface may then be evaluated as equal to $T_0 k/S$ where, hopefully, k may be read off from Table 2. Application of this simple expression to the case already evaluated gives for the heat flow $(29.27 \times 6.1 \times 3.6)/161.26 = 3.98$ cal/cm²/hr which is reasonable in comparison to the given value for $Q(0, 225)$ of 4.55 cal/cm²/hr for, as may be seen from Fig. 2, $T(0, t)$ was decreasing slowly with time at $t = 225$ hours and it would be expected that a constant surface temperature would require a reduced heat flow. A degree of confidence in this procedure is achieved by comparison of the above result with those from chain 40. In this case $T_0 = 20.07°C$, $S = 162.65$ cm and k is taken as 6.0×10^{-3} c.g.s. units from Table 2. The predicted heat flow is 2.65 cal/cm²/hr. From Table 1 the values of $Q(S, t)$ are respectively 2.85 and 1.87 cal/cm²/hr for chains 30 and 40 so that 1.13 and 0.78 cal/cm²/hr are left over to cool the ice. These latter figures should be in ratio to the growth rates which are 0.043 and 0.027 cm/hr. Dividing the heat flows by the growth rates gives 26.3 and 28.8 respectively. The corresponding quotient for chain 10 is 25.0. As thermistor (50.0) was defective, comparison with chain 50 is precluded.

If the rate of ice growth is known, it is possible to break down the heat flow into its components. Consider the data that might be available from a simple study of the situation at chain 20. From Fig. 1 the ice grew 28 cm in 35 days with a mean thickness of 144 cm. During those 35 days the mean surface temperature was about $-21°C$.

The mean rate of growth of the ice is 0.033 cm/hr; T_0 is about 19.5°C giving a temperature gradient of 0.136°C·cm. The heat flow required at the growing interface is $\rho L \times 0.033 + 0.2 = 2.24$ cal/cm²/hr. Taking a value of 6.0×10^{-3} c.g.s. units for the thermal conductivity at the ice surface the total heat flow causing the growth was $6.0 \times 3.6 \times 0.136 = 2.94$ cal/cm²/hr. Thus about 0.70 cal/cm²/hr were required to cool the ice. A check on this calculation is to note that a heat flow into the ice of 2.24 cal/cm²/hr at a gradient of 0.136°C/cm requires a thermal conductivity of 4.5×10^{-3} c.g.s. units which is in good agreement with values given in Table 1.

No particular accuracy is claimed for the immediately preceding calculations, but it is considered that as a simple method for estimation of heat flow through sea ice they are an advance on existing techniques.

The question arises as to what, if any, procedure may be adopted to calculate the transit time through an ice sheet of any thickness from results given here for a sheet 165 cm thick. Schwerdtfeger (1964) has taken the time for a given degree of completion of a temperature change at some fractional depth of the sheet as proportional to S^2, a result based on the study of the transmission of temperature pulses. The present work indicates (section I) that transmission of temperature fluctuations through the sheet is more akin to the propagation of a continuous sinusoidal variation than to that of a pulse, so that transit time directly proportional to S would be predicted. If the sinusoidal analogy were exact the departure of $z=f(t)$ from linearity would be attributable to the variation of K as a function of position. It is probable that transit times in naturally growing ice are proportional to some function of S. At the present stage of knowledge the author would prefer to use the linear relationship for crude scaling purposes.

6. *The thermal constants of sea ice.* In the preceding section information on the thermal conductivity, k, of sea ice has been derived from study of the progression of heat flux along chain 30. An identical analysis may be made of the data presented by any other chain and has been completed satisfactorily for chain 10 which had a large but steady value for $(\partial T/\partial t)$ at the upper surface of the ice at the appropriate scan number (185–87)=98, as may be seen from the air temperature record of Fig. 2. Chain 40 could not be used owing to violent fluctuations of $(\partial T/\partial t)_{z=0}$ around scan (164–87) =77. From the data of chains 30 and 10 values were obtained for thermal conductivities over a range of temperature and salinities.

From the work of Anderson (1960) it is anticipated that k is primarily a function of temperature below $-5°C$ and as there is insufficient data to attempt tabulation as a function of both variables, experimental values for k are tabulated against temperature in Table 3. Theoretical values of k from Anderson (1960) are also shown together with the values for pure ice. Viewing in conjunction with the salinity profile of Fig. 8 the table shows an apparent increase in k for the decrease in salinity at the 45 cm level which is in accordance with theory. It is difficult to arrive at a proper estimate of the accuracy of the experimental values for k presented. Values for the parameters leading to k have been derived from the raw data in a number of ways in an attempt to find limits of confidence and through this experience it is thought that the outside limit of error for k is $\pm 0.2 \times 10^{-3}$ c.g.s. units. The level 165 value for k from chain 30 is within

Table 3. Thermal conductivities (c.g.s. units $\times 10^3$)

Theoretical k*	Expt'l chain 30		Depth in ice cm	Expt'l chain 10		Theoretical k*	Pure ice**	
	k	$T(z)$, °C		$T(z)$, °C	k		Temp. °C	k
6.0	6.2	−30.9	0	−26.1	6.2	5.9	−30	6.09
5.9	6.1	−26.9	15	−23.8	6.1	5.8		
5.8	6.1	−24.0	30	−21.4	6.2	5.8		
5.8	6.2	−21.4	45	−19.3	6.2	5.7	−20	5.80
5.7	6.2	−18.8	60	−17.1	5.9	5.7		
5.6	5.9	−16.3	75	−14.9	5.7	5.6		
5.5	5.8	−13.6	90	−12.7	5.6	5.5		
5.5	5.8	−11.1	105	−10.4	5.4	5.5	−10	5.54
5.4	5.7	− 8.6	120	− 8.1	5.4	5.4		
5.3	5.5	− 6.2	135	− 5.8	5.2	5.2		
5.2	5.2	− 3.8	150	− 3.5	5.0	5.2		
4.7	4.8	− 1.6	165	− 1.6	4.7	4.7	0	5.35

* From Anderson (1960), salinity is constant at 3‰

** Preferred values quoted by Dorsey (1940)

$\pm 0.1 \times 10^{-3}$ c.g.s. units while the corresponding value for chain 10 is less reliable as has already been stated.

Anderson's (1960) values are based on a model (Anderson, 1958) in which sea ice is considered as consisting of pure ice containing isolated spherical brine pockets. More recent work by Schwerdtfeger (1963) included the effect of air bubbles which are always found in ice specimens so that it would be expected that his model would be a better approximation to nature than Anderson's. Schwerdtfeger took a value for k for pure ice of 5.0×10^{-3} c.g.s. units at 0°C in contrast to the value of 5.35×10^{-3} c.g.s. units quoted herein and did not consider variations with temperature. If this new value of k is taken and the proper allowance for temperature variation is made, Schwerdtfeger's analysis, which offers prediction of the thermal conductivity of sea ice down to −8°C, appears to be in quite good agreement with experiment. Both authors are agreed that at low temperatures k for sea ice should approach that of pure ice, a conclusion which is borne out by the present study.

Table 1 shows an increase of k at freezing point with increase rate of growth of ice. According to Adams, French and Kingery (1963) the increased growth rate should result in an increased salinity of the ice at the time of formation. Thus it would appear that k and salinity increase together which is in direct contradiction to the predictions of both Anderson (1960) and Schwerdtfeger (1963). It is well known that brine entrapped in the ice during growth is continually draining down to the interface from higher levels. Kingery and Goodnow (1963) have made quantitive measurement of the phenomenon, in an isolated ice specimen, and Bennington (1963) has observed its effect on crystal growth. As brine drainage occurs at crystal boundaries it is quite possible that the flow of heat associated with it will have little effect on temperature readings made by a localized thermistor. Thus a portion of the heat flow $Q(S, t)$ into the ice would

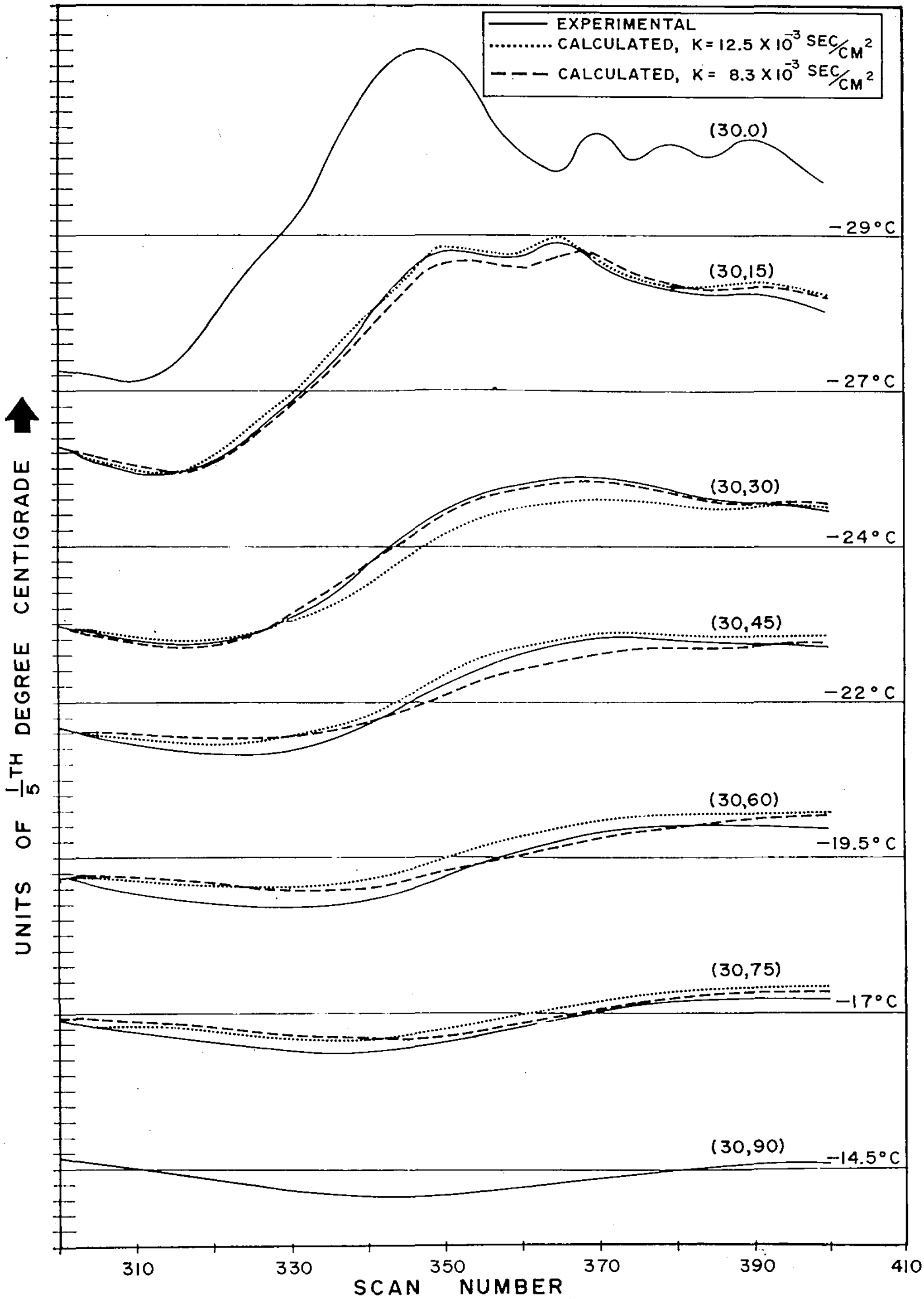

Fig. 9. Comparison of experimental and calculated temperature-time curves. The temperature profile at scan 300 and the curves (30, 0) and (30, 90) are taken as boundary values for the calculations

not be observable as a temperature gradient. As k is defined as the ratio of the heat flow to the temperature gradient, this portion would cause an increase in the effective value of k and the faster the rate of growth the greater the effective value. The work of Weeks and Lee (1962) indicated that sea ice suffers a marked and rapid change in salinity immediately after formation presumably due to drainage. Further discussion awaits quantitative studies of the drainage process at the growing interface.

It should be noted that values given for the thermal conductivity are dependent on the theoretical value for L, the latent heat of formation of sea ice, assumed in the calculation. An experimental determination of L is urgently needed, when, if necessary, values for k could be recalculated from the data given.

At the frequencies of temperature variation typical for a sea ice sheet the propagation of temperature changes is a very insensitive function of the thermal diffusivity. This is illustrated in Fig. 9 where experimental and calculated values for temperatures are shown based on a portion of the data from chain 30 which exhibits a comparatively rapid fluctuation. The calculated curves were drawn by solving the thermal diffusion equation by computer using the temperature profile at scan 300 and the time-temperature curves from (30, 0) and (30, 90) as boundary values. The greatest departures between theory and experiment naturally occur at the central levels. It may be seen that K is changing with temperature but the calculation showed that discrimination of K to within $\pm 1.0 \times 10^{-3}$ cm^2/sec at any level required greater accuracy than was available from the recorded data. It has been noted in section I that the velocity of propagation of a sinusoidal temperature fluctuation through a thick ice sheet is proportional to $(2K\omega)^{\frac{1}{2}}$: Insensitivity to variations in K thus implies insensitivity to variations in frequency and accounts for the possibility of use of the curve $z=f(t)$ as given in Fig. 7 as a general relation to determine the rate of penetration into the ice sheet of surface temperature fluctuations.

Acknowledgments

The author wishes to thank his colleague Mr. P. H. Bridge, and technical staff for invaluable assistance in the operation and maintenance of complex electrical and mechanical equipment under extreme environment conditions. Thanks are also due to the Meteorological office, Department of Transport, for permission to use the official air temperature records from Cambridge Bay N. W. T. and to Dr. K. O. Westphal of this Institute for assistance in data reduction and for the benefit of many helpful discussions.

References

1) ADAMS, C. M., FRENCH, D. N. and KINGERY, W. D. 1963 Field solidification and desalination of sea ice. *In* Ice and Snow (W. D. KINGERY, *ed.*), M. I. T. Press, Cambridge, Mass., 277–288.

2) ANDERSON, D. L. 1958 A model for determining sea ice properties. *In* Arctic Sea Ice, *Nat Acad. Sci.-Nat. Res. Council U.S.A.*, *Publ.* **598**, 148–152.

3) ANDERSON, D. L. 1960 The physical constants of sea ice. *Research*, **13**, 310–318.

4) BENNINGTON, K. O. 1963 Some crystal features of sea ice. *J. Glaciol.*, **4**, 669–688.

5) BRAYTON, G. E. 1962 Station Arlis-I, Oceanography, Part 1, Results 1960 and 1961. Univ. Washington, Dept. of Meteorol. and Climatol. Sci. Rept., Feb. 1962, 20 pp.

6) CARSLAW, H. S. and JAEGER, J. C. 1959 Conduction of Heat in Solids, 2nd Ed., Oxford Univ. Press, 510 pp.

7) DORSEY, N. E. 1940 Properties of Ordinary Water Substance. Reinhold Publ. Corp., 482 pp.

8) KELLEY, J. J., BAILEY, T. and LIESKE, B. J. 1964 Radiative Energy Exchange over Arctic Land and Sea, Part 1, Data 1962, Dept. Atmospheric Sci. Univ. Washington, Sci. Rept, Nov. 1964, 15 pp.

9) KINGERY, W. D. and GOODNOW, W. H. 1963 Brine migration in salt ice. *In* Ice and Snow (W. D. KINGERY, *ed.*), M. I. T. Press, Cambridge, Mass., 237–247.

10) MELLOR, M. 1965 Optical measurements on snow. *CRREL Res. Rept.*, **169**, 1–19.

11) POUNDER, E. R. 1965 The Physics of Ice, Pergammon Press, Oxford, 151 pp.

12) SCHWERDTFEGER, P. 1963 The thermal properties of sea ice. *J. Glaciol.*, **4**, 789–807.

13) SCHWERDTFEGER, P. 1964 The effect of finite heat content and thermal diffusion on the growth of a sea ice cover. *J. Glaciol.*, **5**, 315–324.

14) SCHWERDTFEGER, P. and POUNDER, E. R. 1963 Energy exchange through an annual sea ice cover. *IUGG, Intern. Assoc. Sci. Hydrol., Publ.* **61**, 109–119.

15) UNTERSTEINER, N. 1961 On the mass and heat budget of arctic sea ice. *Arch. Meteorol. Geophys. und Bioklim.*, **A 12**, 2, 151–182.

16) UNTERSTEINER, N. 1964 a Calculations of temperature regime and heat budget of sea ice in the central Arctic. *J. Geophys. Res.*, **69**, 4755–4766.

17) UNTERSTEINER, N. 1964 b Private Communication.

18) VOWINCKEL, E. 1964 Heat flux through the polar ocean ice. Publication in meteorology No. 70. Arctic Meteorol. Res. Group, Dept. of Meteorol., McGill University, Montreal, 15 pp.

19) WEEKS, W. F. and LEE, O. S. 1962 The salinity disiribution in young sea ice. *Arctic*, **15**, 92–108.